GLOBAL ACADEMIC RESEARCH INSTITUTE

COLOMBO, SRI LANKA

GARI International Journal of Multidisciplinary Research

ISSN 2659-2193

Volume: 08 | Issue: 03

On 30th September 2022

http://www.research.lk

Author: Tiranya Illangamudali, Laknee De Silva, Dr. Mathi Kandiah

School of Science, BMS, Sri Lanka

GARI Publisher | Medicinal Plants | Volume: 08 | Issue: 03

Article ID: IN/GARI/ICAS/2022/115 | Pages: 131-152 (22)

ISSN 2659-2193 | Edit: GARI Editorial Team

Received: 15.07.2022 | Publish: 30.09.2022

OBSERVATION OF ANTIOXIDANT, ANTIMICROBIAL AND PHOTOCATALYTIC PROPERTIES OF GREEN SYNTHESIZED SILVER NANOPARTICLES PRODUCED USING EXTRACTS OF COCOS NUCIFERA LEAVES

Tiranya Illangamudali, Laknee De Silva, Dr. Mathi Kandiah

School of Science, BMS, Sri Lanka

ABSTRACT

Antioxidant based research has been on the forefront recently, due to its effects in cancer and aging processes. Silver nanoparticles produced by the green synthesis pathway, has shown to have antioxidant, antimicrobial and photocatalytic properties, enabling them to be used in various medical and industrial applications. In this project, silver nanoparticles were synthesized using coconut leaf extracts of 6 varieties of coconut; ran thambili, porapol, tall typica, gon thambili, green dwarf and bodiri. The nanoparticles were visualized using the UV spectrophotometer in all varieties, where peaks were observed between the wavelengths of 400 nm to 480 nm, optimized at 90°C for 30 mins. A brown colouration observed in the solution caused by the surface plasmon resonance phenomenon indicated the successful synthesis and were identified as semi-conductors. The synthesized nanoparticles were then assessed for their antioxidant properties using the assays, total flavonoid content (TFC), total phenolic content (TPC), total antioxidant content (TAC) and DPPH scavenging assay. Results prove that nanoparticles have a higher antioxidant content compared to their respective water extracts. The photocatalytic activity of 266 ppm and 4000 ppm ran thambili nanoparticle was observed against malachite green dye, under UV and sunlight. The dye was observed to degrade with 266 ppm within 60 mins under UV without catalyst and with 4000 ppm within 120 mins. under sunlight in the presence of catalyst NaBH4. Their antimicrobial activity was observed against Escherichia coli and Staphylococcus aureus. However, no significant difference was observed between the respective water extracts and the nanoparticles. Thus, it can be observed that the produced nanoparticles have various medical and industrial applications.

Keywords: Nanoparticles, antioxidants, coconut leaves, green synthesis

INTRODUCTION

There has been an upsurge in free radicle (FR) and antioxidant-based research, in recent years. FRs are chemical species with an unpaired electron in their final valence shell, which results in their high reactivity and instability. They are produced by various metabolic processes in the body, such as phagocytosis, inflammation and mitochondria, and through various external sources such as (Ultra-violet) UV radiation and X-rays (Perez et al., 2017; Wojtunik-Kulesza et al., 2016). They play significant functions in various metabolic processes such as cellular signalling and blood pressure maintenance. However, increased amounts of FRs in the body results in oxidative stress, which leads to pathogenesis of diseases including

cancers, neurodegenerative diseases and senescence (Teh et al., 2021; Sadeer et al., 2020). The FR levels in the body are regulated by antioxidants under normal conditions.

Antioxidants are capable of remaining stable, even after the removal of an electron, thereby neutralizing excess FRs, by their scavenging activity and controlling the oxidative stress, to maintain homeostasis (Ighodaro and Akinloye, 2017). Antioxidants such as Glutathione and uric acid are endogenous, while others such as carbohydrates and proteins are exogenous (Mironczk-Chodakowska, Witkowska and Zujko, 2018). Due to poor absorption into the cells and disintegration during delivery, clinical trials for synthetic antioxidants have been futile (Vaiserman et al., 2020). The novel nanotechnological approaches have greatly increased the bioavailability and bioactivity of antioxidants. Nanotechnology is the study of unique phenomena of chemical substances at the nanoscale (1-100 nm), allowing for the development of technology with applications in various fields, including medicine, electronics, textile and environment (Maheshwari et al., 2019; Kumar et al., 2020; Behzadi et al., 2015). Nanoparticles (NPs) are nanoscale agglomerates of multiple atoms arranged in a specific manner and are classified based on their physical and chemical properties. Metallic NPs, made of precursors of various metals such as Cu, Au and Ag have various applications, owing to its unique characteristics, resulted by the high surface area to volume ratio. (Altaf et al., 2021). Silver NPs (AgNPs) have various medical applications, due to its antimicrobial properties, and antioxidant properties, and industrial applications due to the photocatalytic properties (Thirumagal and Jeyakumari, 2020; Marimuthu et al., 2022).

Lately there has been an increase in the antimicrobial resistance worldwide, thereby reducing the efficiency of antibiotics. Nokkrut et al. (2019) shows that AgNPs have antimicrobial properties. The Ag+ and Ag0 radicals in NPs, are known to attack bacterial organelles and biomolecules, leading to its destruction. Therefore, AgNPs have been researched in various applications, including wound healing and against food and nosocomial pathogens (Patil and Kim, 2017). Furthermore, textile industry uses AgNPs for their photocatalytic property in order to degrade various dyes.

The significant resistance of the degradation of the organic dyes under aerobic digestion and oxidizing agents contributes to the water scarcity of the world. Previous research proves the capability of degrading azo dyes via the photocatalytic property of AgNPs (Altaf et al., 2021). The excitation of a valence electron of AgNPs by sunlight, results in formation of O2- FRs, thereby attacking azo bonds and degrading the dye. Thus, AgNPs are considered as a more effective method for dye effluent treatment (Marimuthu et al., 2022). The synthesis of AgNPs can be done in several physical, biological and chemical methods based on 2 basic pathways: the top-down pathway (TDP) and the bottom-up pathway (BUP) (Sinsinwar et al., 2018; Kumar et al., 2020). The TDP synthesises NPs by breaking down a bulk substance into the nanoscale by methods such as explosion and laser ablation. The BUP synthesises NPs by assembling atoms in a particular pattern and mostly includes strong reducing agents in techniques such as bioreduction and sol-gel process (Figure 1) (Ovais et al., 2017). The morphology of the NP cannot be controlled when using the TDP. Therefore, in this research BUP is used to synthesize NPs.

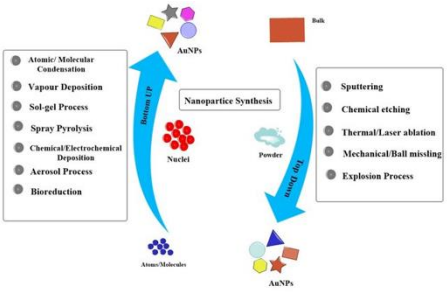

Figure 1: Synthesis of NPs (Ovais et al., 2017)

The AgNPs produced by most chemical processes are unstable, expensive and are producing toxic compounds to the environment. The bioreduction process or the green synthesis process uses phytochemicals in various different parts and products of biological entities, as reducing agents to reduce Ag+ ions into Ag0 (Roy et al., 2019; Kumar et al., 2020). Recently, interest in the use of plant waste for synthesis of AgNPs has increased, owing to its unique physical and chemical properties. In this research, coconut leaves (CLs) are used in the AgNP synthesis.

Coconut (Cocos nucifera L.), belonging to the Arecaceae family, has more than 19 different forms, in 3 varieties found in Sri Lanka (Sinsinwar et al., 2018; Kamral, Perera and Dassanyaka, 2016). In Sri Lanka it is known as 'Kapruka' meaning 'the tree that provides all comforts', because every part of the plant from the root to the flowers and leaves are used for the production of various products (Das et al., 2020). CLs were used since the ancient times, for roofing purposes (Kannaian et al., 2020). However, due to the development of technology, the use of CLs have reduced, making it a waste product (Rashid et al., 2018). Furthermore, NPs have been synthesized from coconut shells, flowers and water have been proved to have antimicrobial and photocatalytic properties (Bello et al., 2016 ;Raj and Arulmozhi, 2014; Elumalai, Kayalvizhi and Silvan, 2014). Further, Manalo et al., 2017 have shown that CLs have antioxidant properties, making it a suitable to be used in this research.

Figure 2: Coconut varieties (A-Porapol (PP), B-Tall typica (TT), C-Ran thambili (RT), D-Bodiri (B), E-Gon thambili (GT), F-Greed dwarf (GD)) (Wijekoon, 2020)

This research aims to synthesize silver nanoparticles (AgNPs) from the water extracts (WEs) of 6 different forms of coconuts (Figure 2) and analyze their shape and size by Scanning Electron Microscope (SEM), perform antioxidant assays such as total Phenolic content (TPC), total flavonoid content (TFC), total antioxidant content (TAC) and (2,2-diphenyl-1-picrylhydrazyl) DPPH assays, antimicrobial assays against Escherichia coli and Staphylococcus aureus via well-diffusion technique, observe its photocatalytic activity against Malachite green dye (MGD) and conductivity. These NPs thus, can be used in the medical and industrial fields based on their properties.

MATERIALS AND METHODOLOGY

Materials

Chemicals	Glassware	Equipment	Biological	Consumables
$AlCl_3$	Beakers (50 ml, 100 ml, 500 ml)	Analytical balance	Coconut leaf samples	Aluminium foil
Ammonium molybdate	Boiling tubes	Autoclave	*Escherichia coli*	Cuvettes
$AgNO_3$	Funnel	Biosafety cabinet	Gentamycin	Eppendorf tubes
Chloroform	Conical flask	Bunsen burner	*Staphylococcus aureus*	Falcon tubes (15 ml, 50 ml)
Conc. H_2SO_4	Glass rod	Burette stand		Micropipette tips
Distilled water	Measuring cylinder	Dry oven		Petri plates
DPPH	Test tubes	Incubator		Pipette tips
Ferric chloride	Watch glass	Micropipette		Swab tubes
Folin reagent		Mortar and pestle		Tissues
HCl		Spatula		Whatman filter paper no. 1
Malachite green dye		UV spectrophotometer		Ziplock bags
Methanol				
Millon's reagent				
Mueller -Hilton agar				
$NaBH_4$				
Na_2CO_3				
Na_2SO_4				
Ninhydrin				
Nutrient agar				
Saline water				

Table 1: Materials table

METHODOLOGY

COSHH forms were filled before starting the project and good laboratory practices were maintained throughout the experiments.

Sample collection

Six sample varieties of CLs; porapol (PP), ran thambili (RT), gon thambili (GT), green dwarf (GD), bodiri (B) and tall typica (TT) were collected from the Coconut Research Institute, Lunuwila.

Active compound extraction from CLs

The sample was placed at 40°C in the hot air oven for 20 hours to dry. 2 g of it was finely chopped, mixed in 50 ml of distilled water (DW) and heated at 95°C for 20 minutes in the hot air oven. The

extract was obtained by filtering the solution using the Whatman filter paper no. 1 (Sebastian, Nangia and Prasad, 2018).

Phytochemical screening

The following phytochemical assays shown in Table 2 were performed on the WEs of the CL samples.

Phytochemical	Methodology	Expected result if positive
Quinones	0.5 ml of conc. H2SO4 was added to 0.5 ml of extract	Red colouration
Tannins	3% ferric chloride was added to 0.5 ml extract	Greenish-blue colouration
Proteins	Few drops of millon's reagent was added to 0.5 ml of extract	Formation of a precipitate
Terpenoids	0.5 ml of chloroform and 0.75 ml of conc. H2SO4 was added to 0.5 ml of extract	Formation of a red membrane
Saponin	0.5 ml of extract was shaken	Foamy layer formation
Amino acid	Few drops of ninhydrin was added to 0.5 ml of extract and heated in a water bath	Purple colouration
Phlobatannins	0.5 ml of HCl was added to 0.5 ml of extract	Red precipitate formation

Table 2: Phytochemical screening (Usunobun et al., 2015; Kannaian et al., 2020; Banu and Cathrine, 2015)

Synthesis of silver nanoparticles

9ml of 1 mM AgNO3 was combined with 1 ml of extract and was placed at 90°C and 60°C for 15, 30, 45 and 60 minutes and 24 hours at room temperature. The absorbance was measured from 320nm to 480nm, to confirm the presence of NPs.

SEM analysis

Approximately 10 ml of 4000 ppm RTNP was poured into an Eppendorf tube, and then centrifuged and the excess water was removed. It was analysed using the SEM in Sri Lanka Institute of Nanotechnology (SLINTEC), Homagama.

Antioxidant content (AC) determination

The following assays were performed to determine the AC of the 15 times diluted WEs (DWE) and the NPs (DNPs).

Total Flavonoid Content (TFC)

The test was done in triplicates. 1.5ml of sample was added to 1.5 ml of 2% AlCl3 of sample and was then incubated in room temperature for 10 minutes. It was

then observed under 415 nm using the UV spectrophotometer with the blank being DW. Quercetin standard curve was used in the calculation (Perera and Kandiah, 2018).

Total Phenolic Content (TPC)

2.5 ml of Folin reagent and 2 ml of Na2CO3 was added to 0.5 ml of sample and incubated for 30 minutes at 37°C. It was then observed under 765 nm, using the UV spectrophotometer, with DW as blank and the concentration was measured using Gallic acid as the standard. This test was performed in triplicates (Perera and Kandiah, 2018).

Total Antioxidant Content (TAC)

3 ml of sample was added to 1 ml of solution consisting of 28 mM Na2SO4, 0.6 M H2SO4 and 4 mM ammonium molybdate in 1:1:1 ratio, and then incubated for 90 minutes. at 90°C. It was then observed under 695 nm, using the UV spectrophotometer. This was performed in triplicates, and the concentration was measured using ascorbic acid as the standard (Perera and Kandiah, 2018).

Single-factor ANOVA was performed between water extracts and NPs of each assay, by Microsoft excel software and bi-valent Pearson correlation, by using IBM spss software was performed, respectively.

DPPH assay

1 ml of 15x DWE and DNP was added to 2 ml of 0.04% DPPH and observed under 517 nm, using the UV spectrophotometer, with methanol as the blank. This assay was performed in triplicates. The equation 1 was used in the calculation of percentage scavenging activity (Kandiah and Chandrasekaran, 2021).

$$\%\ scavenging\ activity = \frac{A_{control} - A_{sample}}{A_{control}} \times 100$$

Equation 1: Percentage scavenging activity (Kandiah and Chandrasekaran, 2021)

Photocatalytic activity (PA)

0.5 ml of NPs was added to 50 ml of 2 mM MGD, and the absorbance was measured after a further 30× dilution, from 320 nm to 700 nm, after being kept under UV and sunlight at 267 ppm and 4000 ppm concentrations. It was then repeated by adding 0.5 ml NP and NaBH4 as a catalyst for both concentrations. The same experiment was performed, with 25 ml of dye for 0.5 ml NaBH4 and both NP concentrations. The rate constant was calculated using the gradient of time vs ln(C/C_0) (Kandiah and Chandrasekaran, 2021).

Antimicrobial Sensitivity Testing

A cotton swab was used to swab the Escherichia coli and Staphylococcus aureus on the Mueller-Hilton agar plates. The plates were divided into four parts and three wells were created. A gentamicin disk was placed, and the wells were filled with duplicates (S1 and S2) of sample and saline solution (Figure 3). They were then incubated for 24 hours under 37°C. The zone of inhibition (ZOI) was then measured. ANOVA test was performed between WE and NP of each bacterial strain and between bacterial strains.

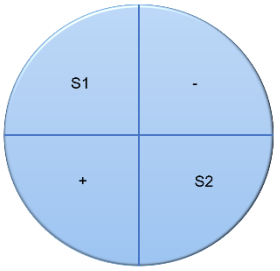

Figure 3: Petri plate labelling (S1, S2 = samples, - = saline solution, + = Gentamicin disk)

RESULTS

Phytochemical Analysis

The 6 WEs of CLs were used in the phytochemical screening. All samples had quinones, proteins, tannins, saponins, phlobatannins and terpenoids and was tested negative for amino acids (table 3).

AgNP synthesis

A colour change observed in Figure 4, indicates the synthesis of NPs.

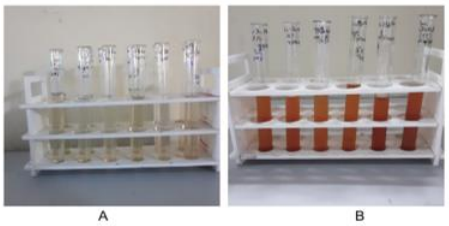

Figure 4: AgNP synthesis (A-before, B-after) at 90°C for 30mins

Test	PP	GD	GT	RT	TT	B	
Quinones	+	+	+	+	+	+	
Proteins	+	+	+	+	+	+	
Tannins	+	+	+	+	+	+	
Amino acids	-	-	-	-	-	-	
Saponins	+	+	+	+	+	+	
Phlobatannins	+	+	+	+	+	+	
Terpenoids	+	+	+	+	+	+	

Table 3: Phytochemical analysis results

When observed under the UV-vis spectrophotometer, peaks were observed between 400-480 nm, which proves the presence of AgNPs (Figure 5).

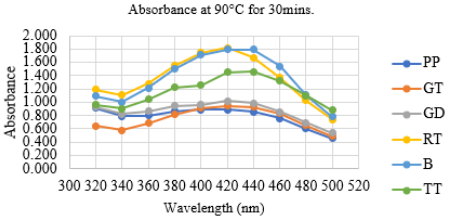

Figure 5: UV spectroscopic results at 90°C at 30 mins

Table 4: Optimization tables

Sample	60°C 15min	60°C 30min	60°C 45min	60°C 60min	90°C 15min	90°C 30min	90°C 45min	90°C 60min	Room temperature
PP	+	+	-	+	+	+	-	+	+
GT	+	-	+	+	+	+	-	+	+
GD	+	+	+	+	+	+	-	+	+
RT	+	+	+	+	+	+	+	+	+
B	+	+	-	-	+	+	+	+	+
TT	+	+	+	+	+	+	+	+	+

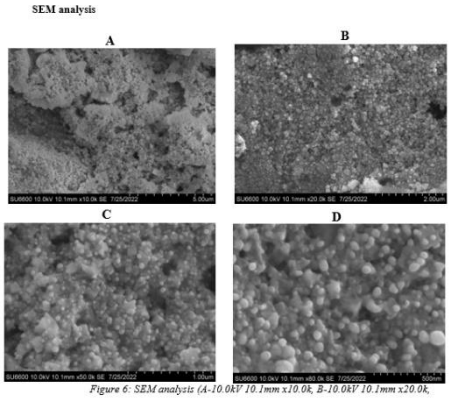

Figure 6: SEM analysis (A-10.0kV 10.1mm x10.0k, B-10.0kV 10.1mm x20.0k, C- 10.0kV 10.1mm x50.0k, D- 10.0kV 10.1mm x80.0k)

Spherical shaped, NPs were observed with an average diameter of 68 nm (Figure 6).

Antioxidant assays

Total Flavonoid Content

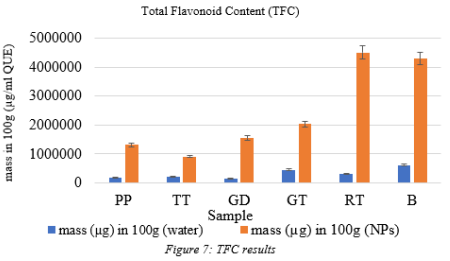

Figure 7: TFC results

AgNPs were observed to have a higher flavonoid content (FC) than the WE (Figure 7).

Table 5: ANOVA test for TFC

ANOVA: Single Factor

Summary						
Groups	Count	Sum	Average	Variance		
Column 1	6	1926041.667	321006.9	3.21E+10		
Column 2	6	14625000	2437500	2.45E+12		
ANOVA						
Source of Variation	SS	df	MS	F	P-value	F crit
Between Groups	1.34386E+13	1	1.34E+13	10.80699	0.008186	4.964602744
Within Groups	1.24351E+13	10	1.24E+12			
Total	2.58738E+13	11				

The P-value was observed to be below 0.05, indicating a significant difference (SD), between the WEs and NPs (Table 5).

Total Phenolic Content

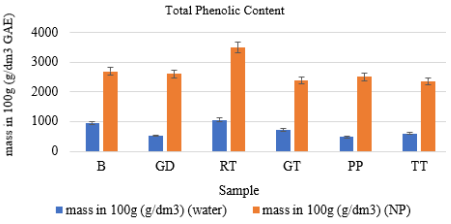

Figure 8: TPC results

The AgNPs had a higher phenolic content (PC) compared to WEs (Figure 8).

Table 6: ANOVA test for TPC

ANOVA: Single Factor

Summary						
Groups	Count	Sum	Average	Variance		
Column 1	6	4346.214286	724.369	55952.22		
Column 2	6	16051.42857	2675.238	175590.1		
ANOVA						
Source of Variation	SS	df	MS	F	P-value	F crit
Between Groups	11417670.12	1	11417670	98.62274	1.69E-06	4.964603
Within Groups	1157711.756	10	115771.2			
Total	12575381.88	11				

The P-value was observed to be less than 0.05, which proves that there is a SD between WEs and NPs (Table 6).

Total Antioxidant Content

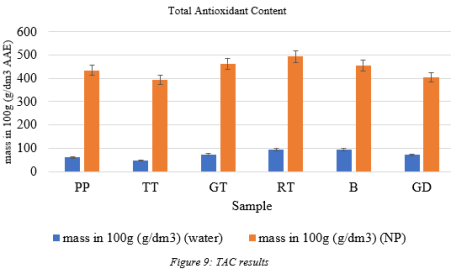

Figure 9: TAC results

The NPs were observed to have a higher AC than the WEs (Figure 9).

Table 7: ANOVA test for TAC

ANOVA: Single Factor

Summary						
Groups	Count	Sum	Average	Variance		
Column 1	6	439.1818182	73.19697	347.7243		
Column 2	6	2644.090909	440.6818	1429.106		
ANOVA						
Source of Variation	SS	df	MS	F	P-value	F crit
Between Groups	405135.3416	1	405135.3	456.0202	1.13E-09	4.964603
Within Groups	8884.153323	10	888.4153			
Total	414019.4949	11				

The P-value was observed to be less than 0.05, indicating a SD between the NPs and WEs (Table 7).

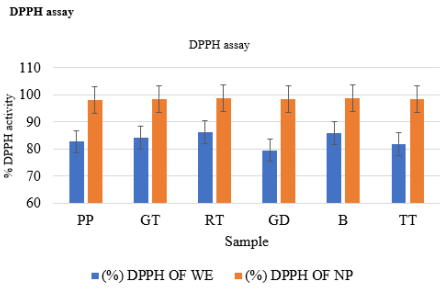

Figure 10: DPPH results

The DPPH scavenging activity of NPs was observed to higher than respective WEs (Figure 10).

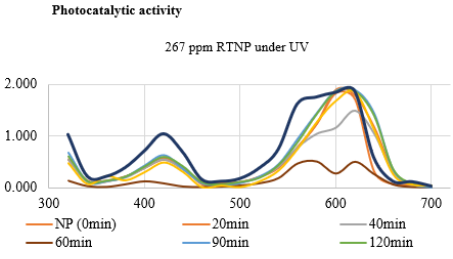

Figure 11: Photocatalytic activity of 267 ppm RTNP under UV

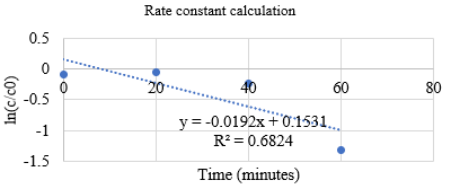

Figure 112: Rate constant calculation (267 ppm RTNP under UV)

Complete degradation of MGD was observed, under UV in the presence of 267 ppm RTNP within 60 minutes (Figure 11), with a rate constant of 0.0192 (Figure 12).

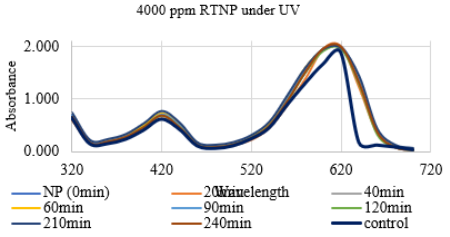

Figure 1312: Photocatalytic activity of 4000 ppm RTNP under UV

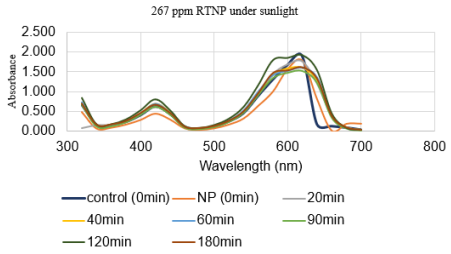

Figure 134: Photocatalytic activity under sunlight for 267 ppm RTNP

No MGD degradation was observed under UV for 4000 ppm RTNP (Figure 13) and under sunlight for 267 ppm RTNP (Figure 14).

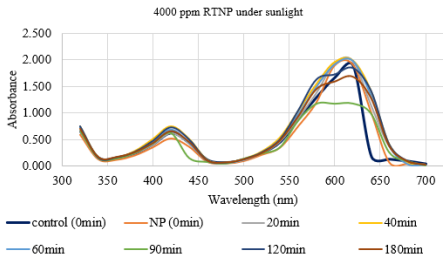

Figure 145: Photocatalytic activity of 4000 ppm RTNP under sunlight

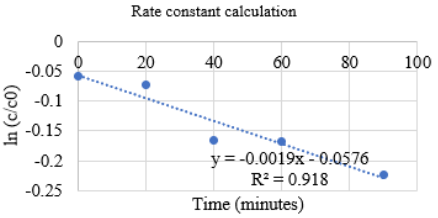

Figure 156: Rate constant calculation for 4000 ppm under sunlight without NaBH4

Partial degradation of MGD was observed under sunlight for 4000 ppm RTNP within 90 minutes (Figure 15) with a rate constant of 0.0019 (Figure 16).

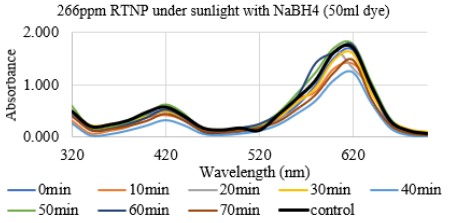

Figure 1716: Photocatalytic activity of 266 ppm RTNP under sunlight with NaBH4 (50 ml dye)

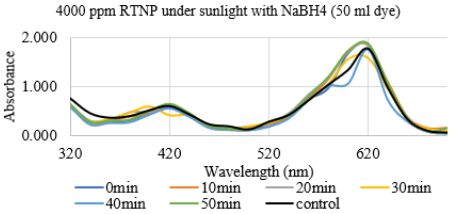

Figure 18: Photocatalytic activity of 4000 ppm RTNP under sunlight with NaBH4 (50 ml dye)

No MGD degradation was observed under sunlight with NaBH4 with 50 ml dye for 266 ppm (Figure 17) or 4000 ppm (Figure 18).

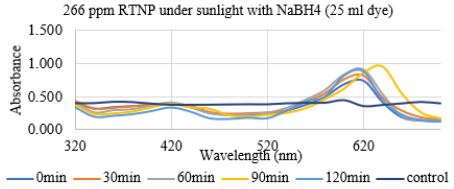

Figure 179: Photocatalytic activity of 266 ppm RTNP under sunlight with NaBH4 (25 ml dye)

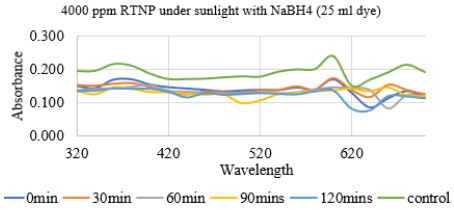

Figure 20: Photocatalytic activity of 4000 ppm RTNP under sunlight with NaBH4 (25 ml dye)

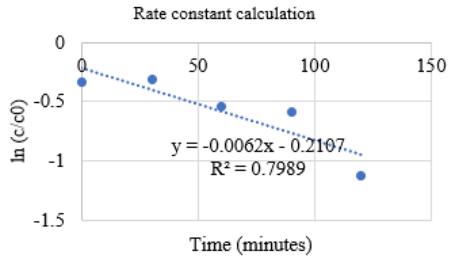

Figure 21: Rate constant for 4000 ppm under sunlight with NaBH4 (25 ml dye)

A complete MGD degradation was observed under sunlight for 4000 ppm with NaBH4 with 25 ml dye (Figure 20) with a rate constant of 0.0062 (Figure 21), but no degradation for 266 ppm (Figure 19).

Antimicrobial assay

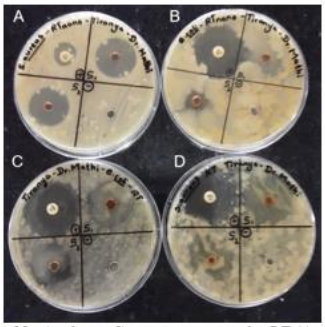

Figure 22: Antibiotic Sensitivity testing for RT (A - RTNP with S.aureus, B - RTNP with E.coli, C - RT water extract with E.coli, D - RT water extract with Staphylococcus aureus)

The ZOI can be observed in the petri plates after 24 hours incubation (Figure 22).

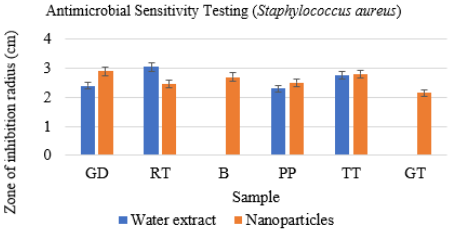

Figure 23: Antimicrobial Sensitivity testing against Staphylococcus aureus

The P-value is greater than 0.5, indicating no SD between the WEs and NPs, against Staphylococcus aureus (Table 8).

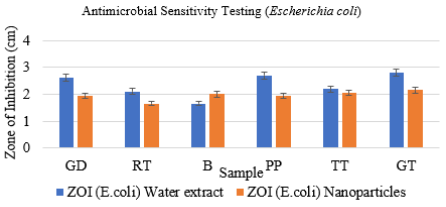

Figure 184: Antimicrobial Sensitivity testing against Escherichia coli

The ZOI of WEs can be observed to be higher compared to NPs, except in B (Figure 24).

Table 8: ANOVA test for anti-microbial sensitivity test between WEs and NPs for Staphylococcus aureus

ANOVA: Single Factor

Summary						
Groups	Count	Sum	Average	Variance		
Column 1	6	10.5	1.75	1.908		
Column 2	6	15.5	2.583333	0.074667		
ANOVA						
Source of Variation	SS	df	MS	F	P-value	F crit
Between Groups	2.083333333	1	2.083333	2.101547	0.177777	4.964603
Within Groups	9.913333333	10	0.991333			
Total	11.99666667	11				

Table 98: ANOVA test for anti-microbial sensitivity test between WEs and NPs for Escherichia coli

ANOVA: Single Factor

Summary						
Groups	Count	Sum	Average	Variance		
Column 1	6	14.05	2.341667	0.192417		
Column 2	6	11.75	1.958333	0.028417		
ANOVA						
Source of Variation	SS	df	MS	F	P-value	F crit
Between Groups	0.440833	1	0.440833	3.992453	0.073619	4.964603
Within Groups	1.104167	10	0.110417			
Total	1.545	11				

The P-value is observed to be higher than 0.05, indicating no SD between WEs and NPs against Escherichia coli (Table 9).

Table 10: ANOVA test for antimicrobial testing between Staphylococcus aureus and Escherichia coli

Summary						
Groups	Count	Sum	Average	Variance		
Column 1	12	26	2.166667	1.090606		
Column 2	12	25.8	2.15	0.140455		
ANOVA						
Source of Variation	SS	df	MS	F	P-value	F crit
Between Groups	0.001667	1	0.001667	0.002708	0.95897	4.30095
Within Groups	13.54167	22	0.61553			
Total	13.54333	23				

The P-value is higher than 0.05, indicating no SD between the AA against the two strains (Table 10).

DISCUSSION

Cancer research and antimicrobial resistance are major concerns in the medical field today, due to its detrimental effect to the human health. AgNPs have shown antioxidant and antimicrobial properties, resulting in an increase in their research. AgNPs were successfully synthesized from 6 varieties of coconut leaf samples, using the green synthesis pathway, though this project, which aims to discover an eco-friendly method for NP synthesis. The 6 samples were mixed with DW and heated at 40°C for 20 mins to extract the active compounds. The heat causes the complex compounds in the leaf to degrade, allowing the active compounds to enter the solution through diffusion. Water is a polar molecule, which allows the extraction of polar active compounds, due to the concentration gradient created. Water was used in this as, it is more polar than ethanol, resulting in a steeper concentration gradient (Lainez-Ceron et al., 2022). Furthermore, water is more eco-friendly than ethanol. It was discovered that all 6 samples had quinones, proteins, tannins, saponins, phlobatannins and terpenoids.

AgNPs are synthesized by the nucleation of Ag0 followed by growth. Ag0 are formed by the reduction of Ag+ by the phytochemicals in the extract. AgNO3 was used as the source of Ag+ (Figure 25) (Ramirez et al., 2019).

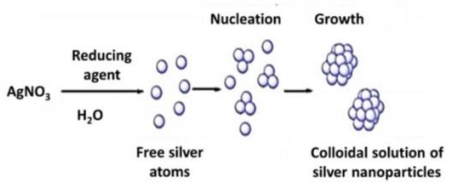

Figure 25: AgNPs synthesis (Ramirez et al., 2019)

Since the synthesis of AgNPs was temperature sensitive, it was observed under different temperatures for varying times, and it was optimized at 90°C for 30 mins, as the highest peak was observed when observing under UV spectrophotometer (Pinero, Camero and Blanco, 2017). A colour change and peaks between the wavelengths 400 to 480 nm, when observed under the UV spectrophotometer was observed confirming the AgNPs synthesis. This was observed due to the surface plasmon resonance phenomenon, which occurs due to the excitation of NPs by UV radiation. The highest absorbance of PP, GD, GT and RT samples were observed at 420 nm, while B and TT showed at 440 nm.

The shape and size of the AgNPs were analyzed by the SEM. It was observed that the synthesized NPs were spherical in shape with an average diameter of 68nm. However, it can be observed that the NPs are of different sizes, giving it a polydisperse nature (Figure 6) (Robertsen et al., 2016). Gomethi et al., reports of 'pseudospherical' shaped NPs with an average diameter of 35nm. The AgNPs produced in this research can be observed to be bigger. Thus, it can be comparatively inefficient in disease treatment, as it can be detected and removed by body's immune mechanisms (Robertsen et al., 2016).

The band gap energy (BGE) required for an electron to jump from the valency electron to the valency band determines the conductivity of the respective NP. It was observed that the lower the BGE, higher the conductivity of the particle. The BGE was measured using Plank's equation (equation 2), where if the BGE was >4eV, it was an insulator, whereas if BGE <3eV it was a semiconductor (Sandeep et al., 2017). NPs of all 6 varieties were classified as semiconductors (Table 11). It can be observed that PP, GT, GD and RT have similar BGEs, while B and TT have a slightly lower BGEs.

$$E = \frac{hc}{\lambda}$$

Equation 2: Plank's equation (E = BGE, h = plank's constant (6.626 × 10−34 Js), λ = wavelength with highest absorbance and c = speed of light (3 × 108 m/s) (Sandeep et al., 2017.)

Table 91: Conductivity table

Sample	BGE in eV	Conductivity
PP	2.95535E-09	semiconductor
GT	2.95535E-09	semiconductor
GD	2.95535E-09	semiconductor
RT	2.95535E-09	semiconductor
B	2.82102E-09	semiconductor
TT	2.82102E-09	semiconductor

Previous research shows that the BGE and NP size are inversely proportional. This can be due to the electron being confined, due to the size reduction, causing the BGE to increase (Singh, Goyal and Devlal, 2018). Therefore, it can be concluded that B and TT have a smaller size. Due to its high semiconductive properties, the produced AgNPs can be used in high-end electronics, such as transistors and optical fibres (Islam, Jacob and Antunes, 2021).

TFC, TPC, TAC and DPPH assays performed helped determine the antioxidant activity of the AgNPs and WEs.

The TFC assay was done based on the calorimetry method, where AlCl3 formed bonds with 4th C ketones and hydroxyl groups in 4th and 5th carbons in flavonoids. The resulting complex provided a maximum absorbance at 432 nm (Figure 26) (Maquasa and Ninsih, 2020). The one-way ANOVA test showed that NPs had a higher FC compared to the respective WEs. This could be because flavonoids acted as the reducing agent of the Ag+ to Ag0. The highest FC of the WE was observed in the order of B>GT>RT>TT>PP>GD and in the NPs, RT>B>GT>GD>PP>TT. Rajesh et al., 2020 showed a total FC of 0.96 mgg-1 in coconut sap compared to the 4.52 mgg-1 observed in GT extract. Thus, it can be observed that the TFC of CLs is lower than in coconut sap.

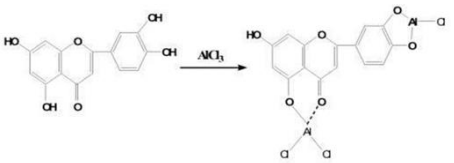

Figure 2619: TFC mechanism (Maquasa and Ninsih, 2020)

The TPC assay uses the FC reagent. It depends on the transfer of electrons from the phenolic compounds to the phosphomolybdate complexes, which causes a colour change detected at 760 nm (Figure 27) (Ford et al., 2019). The one-way ANOVA test showed that NPs had a higher PC compared to their respective WEs. This could be due phenols acting as the reducing agent in NP synthesis. The highest PC was observed in the order of RT>B=GD=PP=TT=GT in NPs, while in WEst RT>B>GT>TT>GD=PP. A total PC of 21.99 mgg-1 was observed in coconut sap in a previous research, compared to 1061.21 gdm-3 in RT extract (Rajesh et al., 2020). Thus, it can be observed that the TPC is lower in CLs in comparison to the coconut sap.

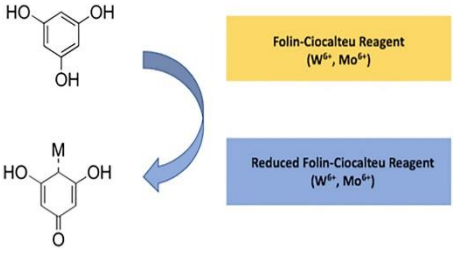

Figure 20: TPC mechanism (Ford et al., 2019)

The TAC assay was performed using the phosphomolybdenum mechanism, where Mo^{6+} ion was reduced to Mo^{5+} by the antioxidants in the extract, resulting in the greenish-blue compound formation. This compound has the optimum detection at 695 nm wavelength (Figure 28) (Sadeer *et al.*, 2020). The ANOVA test performed showed that the AC of NPs were significantly higher in comparison to the WE. The AC of the NPs was observed in the order of RT=GT=B>PP=GD=TT, while in the WE, RT=B>GT=GD=PP>TT was observed. Kannaian *et al.*, 2020 showed a 155.87mg TAE/g in comparison to the 93.67 gdm^{-3} observed in RT extract. Thus, it can be observed that the TAC of CLs is lower than in coconut sap.

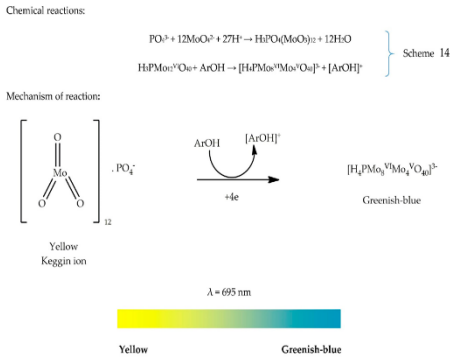

Figure 21: TAC mechanism (Sadeer et al., 2020)

The DPPH assay assesses the rate at which DPPH* reduces to DPPH or DPPH-H, which has an optimum absorbance at 517 nm by accepting a hydrogen atom or an electron from antioxidants. A gradual decolouration from purple to pale yellow was observed based on the amount of antioxidants present (Figure 29) (Sadeer et al., 2020). It was observed that the DPPH SA NPs>WEs, which corresponds to the TFC, TPC and TAC assays. The % SA was observed in the order of RT=GT=B>GD=TT>PP in WEs, while RT=GT>PP=TT>GD=B IN NPs. Kannaian et al., 2020 showed 88% inhibition by coconut sap, compared to 94.76% observed in CLs. Thus, it can be observed that the coconut sap and CLs have approximately similar SA.

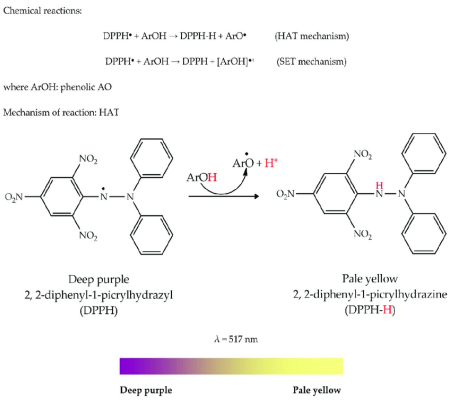

Figure 2922: DPPH mechanism (Sadeer et al., 2020)

Pearson correlation performed on the TFC, TPC and TAC assays, show a strong correlation between TPC and TAC, while showing a moderate correlations between TFC and TAC, and TFC and TPC (Figure 30). Thus, it can be concluded that the TAC is mainly due to the phenols present in the extracts.

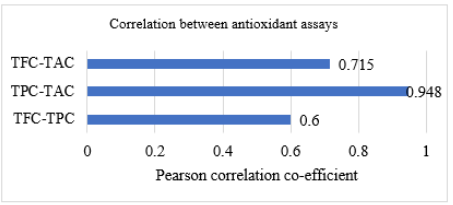

Figure 30: Pearson correlation for antioxidant assays

Previous research have shown that, AgNPs are capable of azo dye degradation. The AgNPs absorb photons in the UV and visible region, which causes the excitation of the electrons on its surface, due to the surface plasmon resonance phenomenon. These electrons reacts with O2 and OH- in the atmosphere and produce free radicles, which react with the dye molecules and degrade them, causing a discolouration (Figure 31)

(Jaffri et al., 2020). MGD was used to observe the PA of RTNP.

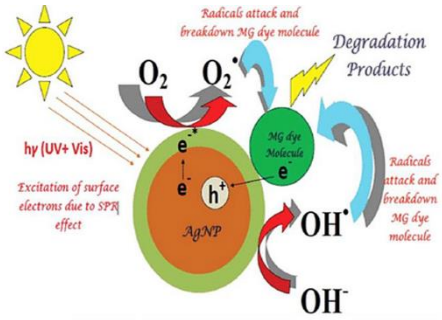

Figure 231: Photocatalytic degradation of malachite green dye (Jaffri et al., 2020)

The highest degradation rate was observed in UV with 266 ppm RTNP, with a rate constant of 0.0192 with 50 ml dye 60 minutes. No degradation was observed with 4000 ppm RTNP under UV, which could because of formation of intermediate substrates. Furthermore, complete degradation was observed under sunlight with 4000 ppm in the presence of catalyst NaBH4 with 25 ml dye, with a rate constant of 0.0062 within 120 minutes. However, no degradation was observed with 266 ppm under similar conditions, could be due to insufficient RTNP in the solution. Degradation was also not observed in dye 50 ml with catalyst in 266 ppm and 4000 ppm RTNP, which could be because the dye concentration was higher than RTNP and NaBH4 concentrations. Moreover, partial degradation was observed in 4000 ppm RTNP under sunlight without NaBH4 with a rate constant of 0.0019, within 90 minutes. This could be because of the formation of intermediate substrates. However, no degradation was observed in 266 ppm RTNP under similar conditions, could be because the concentration of RTNP and NaBH4 was not sufficient. Jaast and Grewal, 2021 had reported that AgNPs from Citrus reticulata peel were able to degrade MG within 120 hours under sunlight in 4000 ppm.

Studies show that AgNPs have antimicrobial properties. However, its mechanism is still under research. It has been identified that AgNPs can lead to disruption of the cell wall, DNA and ribosomal destabilization and reactive oxygen species production leading to obstruction of the cellular pathways, such as cellular respiration, causing cell death (Figure 32) (Patil and Kim, 2017).

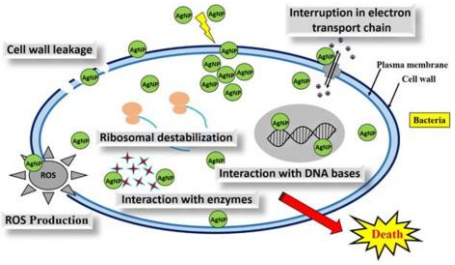

Figure 242: Antimicrobial activity of AgNPs (Patil and Kim, 2017)

Well-diffusion technique was used in this research, to determine the AA of CL NPs against Staphylococcus aureus and Escherichia coli. ZOI was observed in all WEs against Escherichia coli, but only in GD, RT and TT WEs against Staphylococcus aureus. This could be due to the thin peptidoglycan cell wall around Escherichia coli, who are gram-negative compared to Staphylococcus aureus (Bharathi et al., 2018). However, no significant difference was identified between the WEs and the NPs against either organism. Furthermore, no SD was observed between the ZOIs of Staphylococcus aureus and Escherichia coli. Thus, it can be concluded that the AgNPs of CLs does not have an added antimicrobial property.

In conclusion, synthesis of AgNPs from CLs via the green synthesis pathway was successful and was proved by the brown colouration and the peaks observed by the UV-vis spectrophotometer. It was

optimized at 90°C for 30 minutes. The synthesis took place due to the oxidation of the phytochemicals, such as quinones, proteins, tannins, saponins, phlobatannins and terpenoids in the CLs. The SEM analysis showed spherical NPs with 60 nm diameter. The antioxidant assays showed a higher AC in NPs compared to their respective WEs. MGD was degraded under UV within 60 minutes with a rate constant of 0.0192, by 266 ppm RTNP. There was no significant difference between the AA between the WEs and synthesized NPs. Therefore, it can be observed that the CL NPs can be used in the treatment of free radical based diseases and industrially in dye effluent treatment.

REFERENCES

Altaf, N.-U.-H., Naz, M.Y., Shukrullah, S. and Bhatti, H.N. (2021) 'Testing of photocatalytic potential of silver nanoparticles produced through nonthermal plasma reduction reaction and stabilized with saccharides', Main Group Chemistry, ResearchGate [Online]. Available at: http://dx.doi.org/10.3233/MGC-210059 (Accessed date: 19 March 2022).

Banu, K.S. and Cathrine, L. (2015) 'General Techniques Involved in Phytochemical Analysis', International Journal of Advanced Research in Chemical Science (IJARCS), 2 (4), pp. 25-32, Google Scholar [Online]. Available at: https://www.arcjournals.org/pdfs/ijarcs/v2-i4/5.pdf (Accessed date: 28 February 2022).

Behzadi, S., Ghasemi, F., Ghalkeni, M., Askarran, A.A., Akbari, S.M., Pakpour, S., Hormozi-Nezhad, M.R., Jamshid, Z., Mirsadeghi, S., Dinatvand, R., Atyabi, F. and Mahmoudi, M. (2015) 'Determination of nanoparticles using UV-Vis spectra', Nanoscale, 7, pp. 5134-5139, Royal Society of Chemistry [Online]. Available at: https://doi.org/10.1039/C4NR00580E (Accessed date: 1 March 2022).

Bello, S.A., Agunsoye, J.O., Adebisi, J.A., Kolawole, F.O. and Hassan, S.B. (2016) 'Physical properties of coconut shell nanoparticles', Journal of Science, Engineering and Technology, 12 (1), pp. 63-79, ResearchGate [Online]. Available at: https://www.bing.com/ck/a?!&&p=05d473a3a29e4a384baa83695c39f9200da129dbd42fd6f2475f1552a1257685JmltdHM9MTY1NjY5MjA0MyZpZ3VpZD03YzE1ZjBjYy1iNzllLTQ3M2ItYmYyZC0xZDE4MzVjOGI3N2ImaW5zaWQ9NTEzMQ&ptn=3&fclid=d27c37ff-f958-11ec-a57b-f889d8086a80&u=a1aHR0cHM6Ly93d3cucmVzZWFyY2hnYXRlLm5ldC9wdWJsaWNhdGlvbi8zMDU2NTA2MDlfUEhZU0lDQUxfUFJPUEVSVElFU19PRl9DT0NPTlVUX1NIRUxMX05BTk9QQVJUSUNMRVM&ntb=1 (Accessed date: 25 June 2022).

Bharathi, D., Josebin, M.D., Vasantharaj, S. and Bhuvaneshwari, V. (2018) 'Biosynthesis of silver nanoparticles using stem bark extracts of Diospyros montana and their antioxidant and antibacterial activities', Journal of Nanostructure in Chemistry, 8, pp.83-92, SpringerLink [Online]. Available at: https://doi.org/10.1007/s40097-018-0256-7 (Accessed date: 24 July 2022).

Das, G., Shin, H.-S. S., Kumar, A., Vishnuprasad, C.N. and Patra, J.K. (2020) 'Photo-mediated optimized synthesis of silver nanoparticles using the extracts of outer shell fibre of Cocos nucifera L. fruit and detection of its antioxidant, cytotoxicity and antibacterial potential', Saudi Journal of Biological Sciences, 28, pp. 980-987, ScienceDirect [Online]. Available at: https://doi.org/10.1016/j.sjbs.2020.11.022 (Accessed date: 26 February 2022).

Elumalai, E.K., Kalyalvizhi, K. and Silvan, S. (2014) 'Coconut water assisted

green synthesis of silver nanoparticles', Journal of Pharmacy and Bioallied Sciences, 6 (41), Pubmed [Online]. Available at: https://doi.org/10.4103/0975-7406.142953 (Accessed date: 30 June 2022).

Flieger and Flieger (2020) 'The [DPPH●/DPPH-H]-HPLC-DAD method on tracking the antioxidant activity of pure antioxidants and goutweed (Aegopodium podagraria L.) hydroalcoholic extracts', Molecules, 25 (24), MDPI [Online]. Available at: https://doi.org/10.3390/molecules25246005 (Accessed date: 23 July 2020).

Ford, L.L., Theodoridou, K., Sheldrake, G.N. and Walsh, P. (2019) 'A critical review of analytical methods used for the chemical characterization and quantification of phlorotannin compounds in brown seaweeds', Phytochemical Analysis, 30 (4), pp. 1-13, ResearchGate [Online]. Available at: http://dx.doi.org/10.1002/pca.2851 (Accessed date: 17 March 2022).

Gomathi, M., Prakasam, A., Chandrasekaran, R., Gurusubramaniam, G., Revathi, K. and Rajeshkumar, S. (2019) 'Assessment of silver nanoparticle from cocos nucifera (coconut) shell on dengue vector toxicity, detoxifying enzymatic activity and predatory response of aquatic organism', Journal of Cluster Science, 30, pp.1525-1532, SpringerLink [Online]. Available at: https://doi.org/10.1007/s10876-019-01596-7 (Accessed date: 27 July 2022).

Ighodaro, O.M. and Akinloye, O.A. (2017) 'First line defence antioxidants-superoxide dismutase (SOD), catalase (CAT) and glutathione peroxidase (GPX): Their fundamental role in the entire antioxidant defence grid', Alexandria Journal of Medicine, pp. 287-293, ScienceDirect [Online]. Available at: https://doi.org/10.1016/j.ajme.2017.09.001 (Accessed date: 3 March 2022).

Islam, A., Jacob, M.V. and Antunes, E. (2021) 'A critical review on silver nanoparticles, from synthesis and applications to its mitigation through low-cost adsorption by biochar', Journal of Environmental Management, 281, Elsevier [Online]. Available at: https://doi.org/10.1016/j.jenvman.2020.111918 (Accessed date: 4 June 2022).

Jaast, S. and Grewal, A. (2021) 'Green synthesis of silver nanoparticles, characterization and evaluation of their photocatalytic dye degradation activity', Current Research in Green and Sustainable Chemistry, 4, Elsevier [Online]. Available at: https://doi.org/10.1016/j.crgsc.2021.100195 (Accessed date: 31 March 2022).

Jaffri, S.B., Ahmad, K.S., Thebo, K.H. and Rehman, F. (2020) 'Sustainability consolidation via employment of biomimetic ecomaterials with an accentuated photo-catalytic potential: emerging progressions', Reviews in Inorganic Chemistry, ResearchGate [Online]. Available at: 10.1515/revic-2020-0018 (Accessed date: 20 July 2022).

Kamral, L.C.J., Perera, S.A.C.N. and Dassanayaka, P.N. (2016) 'Sri Lanka Yellow Semi Tall; A new addition to the coconut (Cocos nucifera L.) classification in Sri Lanka', Cocos, 22, pp. 49-55, ResearchGate [Online]. Available at: http://dx.doi.org/10.4038/cocos.v22i1.5811 (Accessed date: 2 March 2022).

Kandiah, M. and Chandrasekaran, K.N. (2021) 'Green synthesis of silver nanoparticles using Catharanthus roseus flower extracts and the determination of their antioxidant, antimicrobial and photocatalytic activity', Journal of Nanotechnology, 2021, Hindawi [Online]. Available at:

https://doi.org/10.1155/2021/5512786 (Accessed date: 24 March 2022).

Kannaian, U.P.N., Edwin, J.B., Rajagopal, V., Shankar, S.N. and Srinivasan, B. (2020) 'Phytochemical composition and antioxidant activity of coconut cotyledon', Heliyon, ScienceDirect [Online]. Available at: https://doi.org/10.1016/j.heliyon.2020.e03411 (Accessed date: 27 February 2022).

Kumar, H., Bhardwaj, K., Kuca, K., Kalia, A., Nepovimova, E., Verma, R. and Kumar, D. (2020) 'Flower-based green synthesis of metallic nanoparticles: Applications beyond fragrance', Nanomaterials, 10 (4), MDPI [Online]. Available at: https://doi.org/10.3390/nano10040766 (Accessed date: 6 March 2022).

Lainez-Cerón, E., Ramírez-Corona, N., López-Malo, A. and Franco-Vega, A. (2022) 'An overview of mathematical modeling for conventional and intensified processes for extracting essential oils', Chemical Engineering and Processing - Process Intensification, 178, ScienceDirect [Online]. Available at: 25 July 2022).

Maheshwari, R., Joshi, G., Mishra, D.K. and Tekada, R.K. (2019) 'Bionanotechnology in pharmaceutical research', in Tekade, R.K. (ed.) Basic Fundamentals of Drug Delivery. ScienceDirect [Online]. Available at: https://doi.org/10.1016/B978-0-12-817909-3.00012-1 (Accessed date: 4 March 2022).

Manalo, R.V., Silvestre, M.A., Barbosa, A.L.A. and Medina, P.M. (2017) 'Coconut (Cocos nucifera) ethanolic leaf extract reduces amyloid-β (1-42) aggregation and paralysis prevalence in transgenic Caenorhabditis elegans independently of free radical scavenging and acetylcholinesterase inhibition', Biomedicines, 5 (2), MDPI [Online]. Available at: https://dx.doi.org/10.3390%2Fbiomedicines5020017https://dx.doi.org/10.3390%2Fbiomedicines5020017 (Accessed date: 1 April 2022).

Maquasa, D.A.A. and Ningsih, P. (2020) 'The analysis of total flavonoid levels in young leaves and old soursop leaves (Annona muricata L.) Using UV-vis spectrophotometry methods', Journal of Applied Science Engineering Technology and Education, 2 (1), pp. 11-17, ResearchGate [Online]. Available at: http://dx.doi.org/10.35877/454RI.asci2133 (Accessed date: 17 March 2022).

Marimuthu, S., Antonisamy, A.J., Malayandi, S., Rajendran, K., Tsai, P.-C, Pugazhendhi, A., Ponnusamy, V.K. (2020) 'Silver nanoparticlesin dye effluent treatment: A review on synthesis, treatment methods, mechanisms, photocatalytic degradation, toxic effects and mitigation of toxicity', Journal of Photochemistry and Photobiology, 205, ScienceDirect [Online]. Available at: https://doi.org/10.1016/j.jphotobiol.2020.111823 (Accessed date: 26 March 2022).

Mironczk-Chodakowska, I., Witkowska, A.M. and Zujko, M.E. (2018) 'Endogenous non-enzymatic antioxidants in the human body', Advances in Medical Sciences, 63 (1), pp. 68-78, ScienceDirect [Online]. Available at: https://doi.org/10.1016/j.advms.2017.05.005 (Accessed date: 3 April 2022).

Morbagheri, V.S., Alizadeh, E., Elahi, M.Y. and Bahabadi, S.E. (2018) 'Phenolic content and antioxidant properties of seeds from different grape cultivars grown in Iran', Natural Product Research, 32 (4), pp. 425-429, Taylor and Francis Online [Online]. Available at: https://doi.org/10.1080/14786419.2017.1306705 (Accessed date: 23 July 2020).

Nokkrut, B.-O., Pisuttipiched, S., Khantayanuwong, S. and Puagsin, B. (2019) 'Silver nanoparticle-based

paper packaging to combat black anther disease in orchid flowers', Coatings, 9 (1), MDPI [Online]. Available at: https://doi.org/10.3390/coatings9010040 (Accessed date: 2 March 2022).

Ovais, M., Raza, A., Naz, S., Islam, N.U., Khalil, A.T., Ali, S., Khan, M.A. and Shinwari, Z.K. (2017) 'Current state and prospects of the photosynthesized colloidal gold nanoparticles and their applications in cancer therapeutics', Applied Microbiology and Biotechnology, 101, pp. 3551-3565, Springer Link [Online]. Available at: https://doi.org/10.1007/s00253-017-8250-4 (Accessed date: 6 March 2022).

Patil, M.P. and Kim, G.-D. (2017) 'Eco-friendly approach for the nanoparticles synthesis and mechanism behind antibacterial activity of silver and anticancer activity of gold nanoparticles', Applied Microbiology and Biotechnology, 101 (1), pp. 79-92, ResearchGate [Online]. Available at: https://link.springer.com/article/10.1007%2Fs00253-016-8012-8 (Accessed date: 19 March 2022).

Penprapai, P. and Intharit, S. (2017) 'Total phenolic content and antioxidant activity of coconut oil enriched with some extracts of curcuma species in Thailand', The Journal of Applied Sciences, 16, pp. 48-64, ResearchGate [Online]. Available at: 10.14416/j.appsci.2017.10.S07 (Accessed date: 24 July 2020).

Perera, B.R. and Kandiah, M. (2018) 'Microwave assisted one-pot green synthesis of silver nanoparticles using leaf extracts from Vigna unguiculate: Evaluation of antioxidant and antimicrobial activities', International Journal of Multidisciplinary Studies (IJMS), 5 (2), pp. 62-78 [Online]. Available at: https://doi.org/10.31357/ijms.v5i2.3968 (Accessed date: 1 March 2022).

Perez, A.L.Z., Zuniga-Gonzalez, G.M., Gomez-Meda, B.C., Lazalde-Ramos, B.P., Ortiz-Garcia, Y.M., Morales-Velazquez, G., Velazquez, C.G. and Sanchez-Prada, M.G. (2017) 'Periodontal disease and nuclear and oxidative DNA damage', Insights into Various Aspects of Oral Health, ResearchGate [Online]. Available at: http://dx.doi.org/10.5772/intechopen.68446 (Accessed date: 3 March 2022).

Piñero, S., Camero, S. and Blanco, S., 2017. Silver nanoparticles: Influence of the temperature synthesis on the particles' morphology. Journal of Physics: Conference Series, 786, ResearchGate [Online]. Available at: 10.1088/1742-6596/786/1/012020 (Accessed date: 23 July 2022).

Raj, N. and Arulmozhi, K. (2014) 'Synthesis of Nanoparticles from Coconut Flower', International Journal for Scientific Research and Development, 2 (10) [Online]. Available at: https://www.bing.com/ck/a?!&&p=d63ec74bb5d489790e6f0b179b38e7f946253ec55d24ffbc08b322452bdf6034JmltdHM9MTY1NjY5MjA0MyZpZ3VpZD03YzE1ZjBjYy1iNzllLTQ3M2ItYmYyZC0xZDE4MzVjOGI3N2ImaW5zaWQ9NTIzMw&ptn=3&fclid=d27dc2a6-f958-11ec-b746-2839161cc683&u=a1aHR0cHM6Ly93d3cuaWpzcmQuY29tL2FydGljbGVzL0lKU1JEVjJJMTAwNjIucGRm&ntb=1 (Accessed date: 26 June 2022).

Rajesh, M.K., Muralikrishna, K.S., Nair, S.S., Krishna, B., Kumar, Subrahmanya, T.M., Sonu, K.P., Subaharan, K., Sweta, H., Keshava, Prasad, Neeli, Chadran, Karunasagar, I., Hebbar, K.B. and Karun, A. (2020) 'Facile coconut inflorescence sap mediated synthesis of silver nanoparticles and its diverse antimicrobial and cytotoxic properties', Materials Science and Engineering, 111, Elsevier [Online]. Available at: https://doi.org/10.1016/j.msec.2020.110834 (Accessed date: 4 June 2022).

Ramirez, J.F., Ortiz, J., Cuellar, J.A., Neranjo, C.A., Jimenez, F.N. and Londono, O.M. (2019) 'Synthesis of colloidal silver nanoparticles and their bactericidal effects on E.coli, S. epidermidis and oral plaque', Journal of Physics: Conference Series, 1541 (1), ResearchGate [Online]. Available at: http://dx.doi.org/10.1088/1742-6596/1541/1/012017 (Accessed date: 5 June 2022).

Rashid, R.A., Jawad, A.H., Ishak, M.A.B.M. and Kasim, N.N. (2018) 'FeCl3-activated carbon developed from coconut leaves: characterization and application for methylene blue removal', Sains Malaysiana, 47 (3), pp. 603–610, ResearchGate [Online]. Available at: http://dx.doi.org/10.17576/jsm-2018-4703-22 (Accessed date: 3 March 2022).

Robertson, J., Rizzello, L., Avila-Olias, M., Gaitzsch, J., Contini, C., Magon, M.S., Renshaw, S.A. and Battaglia, G. (2016) 'Purification of nanoparticles by size and shape', Scientific Reports, 6, Nature [Online]. Available at: https://doi.org/10.1038/srep27494 (Accessed date: 27 July 2022).

Roy, A., Some, S., Mandal, A.K. and Yamaz, M.D. (2019) 'Green synthesis of silver nanoparticles: Biomolecule-nanoparticle organizations targeting antimicrobial activity', RSC Advances, 9, Royal Society of Chemistry [Online]. Available at: https://doi.org/10.1039/C8RA08982E (Accessed date: 4 March 2022).

Sadeer, N.B., Montesano, D., Albrizio, S., Zengin, G. and Mahomoodally, M.F. (2020) 'The Versatility of Antioxidant Assays in Food Science and Safety—Chemistry, Applications, Strengths, and Limitations', Antioxidants, 9 (8), MDPI [Online]. Available at: https://doi.org/10.3390/antiox9080709 (Accessed date: 17 March 2022).

Sandeep, D., Kumar, T.V., Rao, P.S.S., Ravikumar, R.V.S.S.N. and Krishna, A.G. (2017) 'Green synthesis and characterization of Ag nanoparticles from Magnifera indica leaves for dental restoration and antibacterial applications', Progress in Biomaterials, 6, pp.57-66, Pubmed [Online]. Available at: https://doi.org/10.1007%2Fs40204-017-0067-9 (Accessed date: 4 June 2022).

Sebastian, A, Nangia, A. and Prasad, M.N.V. (2018) 'A green synthetic route to phenolics fabricated magnetite nanoparticles from coconut husk extract: Implications to treat contaminated water and heavy metal stress in Oryza sativa L., Journal of Cleaner Production, 174, pp.355-366, ScienceDirect [Online]. Available at: https://doi.org/10.1016/j.jclepro.2017.10.343 (Accessed date: 19 February 2022).

Singh, M., Goyal, M. and Devial, K. (2018) 'Size and shape effects on the band gap of semiconductor compound nanomaterials', Journal of Toibah University for Science, 12 (4), pp.470-475, Taylor and Francis Online [Online]. Available at: https://doi.org/10.1080/16583655.2018.1473946 (Accessed date: 10 June 2022).

Sinsinwar, S., Sarkar, M.K., Suriya, K.R., Nithyanand, P. and Vadivel, V. (2018) 'Use of agricultural waste (coconut shell) for the synthesis of silver nanoparticles and evaluation of their antibacterial activity against selected human pathogens', Microbial Pathogenesis', 124, pp. 30-37, ScienceDirect [Online]. Available at: https://doi.org/10.1016/j.micpath.2018.08.025 (Accessed date: 20 February 2022).

Teh, S.S., Mah, S.H., Lau, H.L.N., Teng, K.T. and Loganathan, R. (2021) 'Antioxidant potential of red palm-pressed mesocarp olein', Journal of Oleo Science, 70 (12), pp. 1719-1729, PubMed [Online]. Available at: https://doi.org/10.5650/jos.ess21147 (Accessed date: 28 February 2022).

Thirumagal, N. and Jeyakumari, A.P. (2020) 'Photocatalytic and antibacterial activity of silver nanoparticles (AgNPs) using palm (Borassus flabellifer L.) water (Pathaneer)', Indian Journal Of Science And Technology, 13 (18), pp. 1856-1866 [Online]. Available at: https://doi.org/10.17485/IJST/v13i18.222 (Accessed date: 26 February 2022).

Usunobun U., Okolie N. P., Anyanwu O. G., Adegbegi A.J., Egharevba M. E. (2015), 'Phytochemical screening and proximate composition of Annona muricata leaves', European Journal of Botany Plant Science and Pathology, 2 (1), pp.18-28, ResearchGate [Online]. Available at: https://www.researchgate.net/publication/279529709_PHYTOCHEMICAL_SCREENING_AND_PROXIMATE_COMPOSITION_OF_ANNONA_MURICATA_LEAVES (Accessed date: 27 February 2022).

Vaiserman, A., Koliada, A., Zayachikivska, A. and Lushchak, O. (2020) 'Nanodelivery of natural antioxidants: An anti-aging perspective', Frontiers in Bioengineering and Biotechnology, 7 [Online]. Available at: https://www.frontiersin.org/article/10.3389/fbioe.2019.00447 (Accessed date: 29 March 2022).

Wijekoon, R. (2014) 'Traditional coconut varieties of Sri Lanka', ResearchGate [Online]. Available at: (PDF) Traditional Coconut Varieties of Sri Lanka (researchgate.net) (Accessed date: 25 February 2022).

Wojtunik-Kulesza, K.A., Oniszczuk, A., Oniszczuk, T. and Waksmundzka-Hajnos, M. (2016) 'The influence of common free radicals and antioxidants on development of Alzheimer's Disease', Biomedicine and Pharmacotherapy, 78, pp. 39-49, ScienceDirect [Online]. Available at: http://dx.doi.org/10.1016/j.biopha.2015.12.024 (Accessed date: 3 March 2022).